

Reinvestigation of the Branching Ratio of the CN + O₂ Reaction

Wenhui Feng and John F. Hershberger*

Department of Chemistry and Molecular Biology, North Dakota State University, Fargo, North Dakota 58105

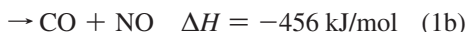
Received: December 23, 2008; Revised Manuscript Received: February 24, 2009

The reaction of the CN radical with O₂ was studied using infrared diode laser absorption spectroscopy. Detection of NO and secondary N₂O products was used to directly measure the product branching ratio. After consideration of possible secondary chemistry and comparison to kinetic modeling simulations, the branching ratio of the CN + O₂ reaction into the NO + CO channel was determined to be $\varphi(\text{NO} + \text{CO}) = 0.20 \pm 0.02$, with little or no temperature dependence over the range 296–475 K.

1. Introduction

The kinetics and dynamics of the CN + O₂ reaction have been extensively studied by both experimental^{1–18} and computation methods.^{19–22} This reaction is an example of a radical–radical reaction proceeding on an attractive potential energy surface without an entrance channel barrier to a deep well, the NCOO intermediate.^{16,23} Several groups have measured total rate constants over the impressive temperature range of 13–3800 K, with a value at 298 K of $2.3 \times 10^{-11} \text{ cm}^3 \text{ molecule}^{-1} \text{ s}^{-1}$.^{4–15}

The product branching ratio of this reaction has also received considerable attention.^{2,17,24,25} Two channels have been previously identified as having significant contributions:



In previous work, estimates of the branching ratio of channel 1b have ranged from 0.06 to 0.29. Previous studies in our laboratory, based on infrared absorption measurements of the CO product yield upon photolysis of ICN/O₂/CF₄ mixtures, have concluded that $\varphi_{1b} = 0.22 \pm 0.02$ at 298 K, with a significant decrease as the temperature is increased.¹⁷ A third product channel, leading to N + CO₂, was found to be insignificant.¹⁷

One serious potential difficulty with previous studies is the possible presence of secondary chemistry, especially the reaction



This has given rise to some question as to whether the previously determined values of φ_{1b} are reliable. Although reaction 1a has been studied in single-collision molecular beam experiments,¹⁸ only the channel 1a products were detected. All experiments involving detection of channel 1b products are bulb experiments. Adding to the uncertainty is the fact that moderate-level ab initio calculations by Mohammad et al. have shown that the most obvious pathway to 1b via a four-center transition state has a high energy barrier, inconsistent with experimental observations.²⁵ This observation led Mohammad et al. to speculate that CO + NO is formed in 1b by a dynamic mechanism in which NCO + O are initially formed with NCO

rotational excitation, followed by 180° NCO rotation and N-atom abstraction as the complex dissociates.²⁵ We note that this proposed mechanism is quite similar to the roaming atom mechanism recently proposed for formaldehyde dissociation.^{26–30} If true, it represents another interesting example of product formation that does not proceed through a classical transition state. Dynamical studies of reaction 1a do support the notion that the NCO products have a high degree of nascent rotational excitation.¹⁸ On the other hand, more recent high-level calculations have found an alternate, lower-energy pathway to CO + NO products via successive rearrangements involving three-center intermediates,²² so a roaming atom mechanism need not necessarily be invoked in order to explain this product channel.

In principle, there are several ways to distinguish between 1b and 2. For example, CO formation from reaction 2 would have a much slower risetime than CO formed in 1b, because under our typical conditions, $[\text{O}_2] \sim 10^{16} \text{ molec cm}^{-3}$, whereas $[\text{O}] \sim 10^{13}$. Our experimental technique, however, directly measures CO by a $\nu = 0 \rightarrow \nu = 1$ rotation–vibration transition, and these reactions produce CO in a wide variety of vibrational quantum states. Vibrational relaxation, accomplished by collisions with CF₄ buffer gas, occurs on only a ~ 50 – $100 \mu\text{s}$ time scale, much slower than the actual reaction 1a. As a result, we maintain that examination of transient signal risetimes is not necessarily an effective way to distinguish between reactions 1b and 2.

In our previous study,¹⁷ we used the following technique to conclude that the contribution of reaction 2 to our CO absorption signals was minor: Different pressures of SiH₄ were included in the reaction mixture. The following additional reactions can then occur:



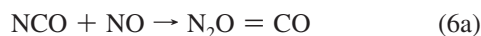
At moderate SiH₄ pressures, any NCO produced in channel 1a would react with SiH₄, thus quenching any CO formation in 1b. Although CN also reacts quickly with SiH₄, quenching of CN radicals involves a competition between SiH₄ and O₂, whereas quenching of NCO radicals involves a competition between SiH₄ and O. Because $[\text{O}] \ll [\text{O}_2]$, these effects are separable. Kinetic modeling of this system predicted that a curve of CO yield vs $[\text{SiH}_4]$ would decay very quickly if reaction 2

* To whom correspondence should be addressed. E-mail: john.hershberger@ndsu.edu.

were the primary source of CO (case A), but more slowly if the CO originated from 1b (case B). The experimental data were consistent with case B, leading to the conclusion that channel 1b was real.

The kinetic modeling used in the study of ref 17 was critically dependent on several rate constants, especially that of the $\text{NCO} + \text{O}$ reaction, which is quite difficult to measure accurately. That study used the then-available value of $k_2 = 7.0 \times 10^{-11} \text{ cm}^3 \text{ molec}^{-1} \text{ s}^{-1}$. Since then, however, McDonald et al. performed a detailed study of reaction 2 and obtained a substantially greater value of $k_2 = 2.1 \times 10^{-10} \text{ cm}^3 \text{ molec}^{-1} \text{ s}^{-1}$.³¹ The effect of this change is to substantially complicate the approach used in our previous study,¹⁷ because a faster value of k_2 means that a greater amount of SiH_4 is required to quench reaction 2. As a result, the modeled CO yield vs $[\text{SiH}_4]$ curves for the two cases A and B become closer together, although still far from identical. The experimental data are still better fit by case B, but the more recent measurement of k_2 has sufficiently reduced our confidence in the conclusions of our earlier report to warrant further study.

The essential difficulty with the approach of reference 17 is that the SiH_4 quenching gas reacts with CN faster than NCO, but we prefer a quencher that will remove NCO much faster than CN. As far as we know, no hydrocarbon or silane will accomplish this. One molecule that will do this, however, is nitric oxide:



At low total pressures, reaction 5 is very slow, with $k_5 = 1.35 \times 10^{-12} \text{ cm}^3 \text{ molec}^{-1} \text{ s}^{-1}$ at 298 K and 30 Torr pressure.³² Reaction 6a is much faster, however, with $k_6 = 3.4 \times 10^{-11} \text{ cm}^3 \text{ molec}^{-1} \text{ s}^{-1}$, and produces channel 6a with a product branching ratio of $\varphi_{6a} = 0.44$.²⁴ Thus, a small amount of NO will not significantly compete for CN radicals, but will effectively quench NCO and, therefore, the secondary chemistry of reaction 2. This approach leads to much better separation in the kinetic modeling of cases A and B. Of course, we cannot use this approach if we are detecting CO formation, because reaction 6a produces CO. We can, however, use isotopically labeled $^{15}\text{N}^{18}\text{O}$ reagents, and then, without spectroscopic interference, probe $^{14}\text{N}^{16}\text{O}$ formation due to 2, 1b, or both. This is the approach used in the present study.

2. Experimental

The experimental setup uses infrared laser absorption spectroscopy using lead salt diode lasers (Laser Components), and has been described in previous publications.^{33,34} CN radicals were produced by 266-nm photolysis of ICN. IR and UV light were collimated and passed through a single-pass 143 cm absorption cell, and the infrared light was detected by a 1-mm-diameter InSb detector (Cincinnati Electronics, $\sim 1 \mu\text{s}$ response time). Transient infrared absorption signals were collected upon photolysis of a reaction mixture and signal-averaged on a digital oscilloscope. Signal averaging was generally limited to ~ 2 – 4 laser shots to avoid significant buildup of reaction products. To account for small probe laser thermal deflection effects, transient signals were collected with the diode laser slightly detuned off

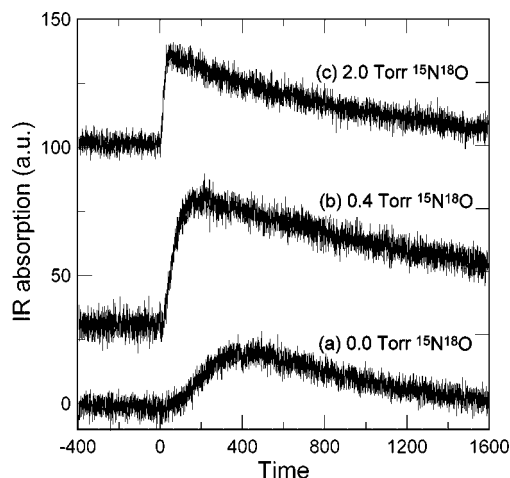
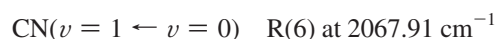


Figure 1. Transient infrared absorption signals for detection of $^{14}\text{N}^{16}\text{O}$ as a function of time (μs), at several different $^{15}\text{N}^{18}\text{O}$ pressures: (a) $P(^{15}\text{N}^{18}\text{O}) = 0$ Torr, (b) $P(^{15}\text{N}^{18}\text{O}) = 0.4$ Torr, (c) $P(^{15}\text{N}^{18}\text{O}) = 2.0$ Torr. Other reagents: $P(\text{ICN}) = 0.20$ Torr, $P(\text{O}_2) = 2.0$ Torr, $P(\text{SF}_6) = 2.0$ Torr.

the spectroscopic absorption lines, and such transients were subtracted from the on-resonant signals.

The HITRAN molecular database³⁵ was used to locate and identify the spectral lines of NO, N_2O product molecules, and CN radicals at



ICN (Aldrich) was purified by vacuum sublimation to remove dissolved air. $^{15}\text{N}^{18}\text{O}$ (Isotec) was purified by repeated freeze–pump–thaw cycles at 153 K to remove NO_2 and N_2O . SF_6 (Matheson) was purified by repeated freeze–pump–thaw cycles at 77 K.

Typical experimental conditions were $P(\text{ICN}) = 0.2$ Torr, $P(\text{O}_2) = P(\text{SF}_6) = 2.0$ Torr, $P(^{15}\text{N}^{18}\text{O}) = 0.5$ Torr, and laser pulse energies of 4 mJ. Under these conditions, we estimate an initial radical yield of $[\text{CN}]_0 \sim 3.0 \times 10^{13} \text{ molecule cm}^{-3}$. SF_6 was used as a buffer gas for detection of NO and N_2O products. The choice of buffer gas was motivated by the desire to relax any nascent vibrationally excited product molecules to a Boltzmann distribution.³³

3. Results and Discussion

3.1. Product Detection. Figure 1 shows transient absorption signals for $^{14}\text{N}^{16}\text{O}$ products upon photolysis of $\text{ICN}/\text{O}_2/^{15}\text{N}^{18}\text{O}/\text{SF}_6$ mixtures. As shown, in the absence of added $^{15}\text{N}^{18}\text{O}$ reagent, the $^{14}\text{N}^{16}\text{O}$ signal has a very long risetime of 400 μs , followed by a slow decay. If $^{15}\text{N}^{18}\text{O}$ reagent is added to quench NCO radical formed in reaction 1a, the observed $^{14}\text{N}^{16}\text{O}$ signal displays a faster risetime. This effect may be partly due to the slower kinetics of reaction 2; however, another likely possibility is that NO is formed in highly vibrationally excited states in reactions 1a and 2. Because we are detecting NO using a $\nu = 0 \rightarrow \nu = 1$ transition, the signal risetime is more indicative of vibrational relaxation kinetics rather than the reaction rates of 1a and 2. The data in Figure 1 suggests that $^{15}\text{N}^{18}\text{O}$ is an efficient

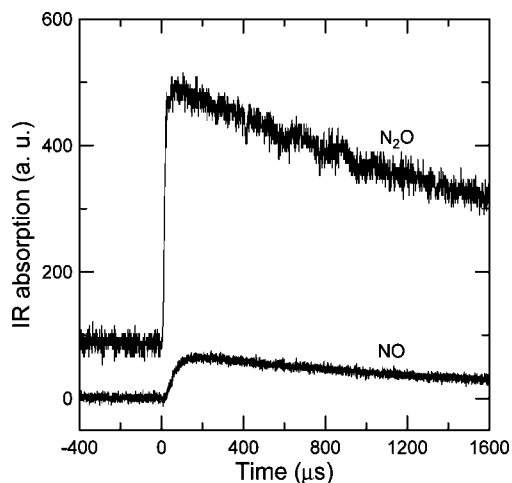


Figure 2. Transient infrared absorption signals of NO and N₂O detected upon 266 nm laser photolysis of reactant mixture: $P(\text{ICN}) = 0.20$ Torr, $P(\text{O}_2) = 2.0$ Torr, $P(\text{SF}_6) = 2.0$ Torr, $P(^{15}\text{N}^{18}\text{O}) = 0.5$ Torr (only for NO signal), and $P(\text{NO}) = 0.5$ Torr (only for N₂O signal).

TABLE 1: Product Branching Ratios of the CN + O₂ Reaction at 296 K

product channel	branching ratio
NCO + O	$\Phi_{1a} = 0.80 \pm 0.02$
CO + NO	$\Phi_{1b} = 0.20 \pm 0.02$

relaxer of ¹⁴N¹⁶O vibrational excitation, causing the signals to display a faster risetime as ¹⁵N¹⁸O increases. This is reasonable because the vibrational frequencies of ¹⁴N¹⁶O and ¹⁵N¹⁸O are sufficiently similar for near-resonant ν - ν energy transfer.

Figure 2 shows typical transient signals of both detected products. The upper trace shows N₂O products produced upon photolysis of ICN/O₂/¹⁴N¹⁶O/SF₆ mixtures. N₂O formation is attributed to reaction 1a followed by 6a. Because an excess of NO is used, we expect virtually all NCO radicals produced in 1a to react with NO. The branching ratio into channel 6a is known,²⁴ $\varphi_{6a} = 0.44$, so that $[\text{NCO}] = [\text{N}_2\text{O}]/0.44$. The lower trace shows the transient signal for ¹⁴N¹⁶O detection upon photolysis of a ICN/O₂/¹⁵N¹⁸O/SF₆ mixture. As will be shown by kinetic simulations (next section), the pressure of ¹⁵N¹⁸O (0.5 Torr) used is sufficient to remove NCO molecules through reaction 6a and, therefore, completely suppresses reaction 2: ¹⁴N¹⁶O formation is therefore attributed solely to reaction 1b.

The slow decay portions of the absorption signals were fit to an exponential function. (Although diffusion decay does not strictly follow exponential behavior, the approximation is sufficient for our purposes.) This exponential was extrapolated to $t = 0$ to obtain signal amplitudes. This is usually only a small correction (~ 5 – 15%) to the peak–peak amplitudes, but the correction increases for the slow-rising signals obtained at very low [¹⁵N¹⁸O]. These extrapolated signals were converted into absolute number densities using tabulated line strengths from the HITRAN database³⁵ and equations described previously.²⁴ Comparing the number densities of NO and NCO results in the branching ratio of φ_{1a} and φ_{1b} , as shown in Table 1. The value $\varphi_{1b} = 0.20 \pm 0.02$ (uncertainty is 1σ) at 296 K is in excellent agreement with our previous measurement.¹⁷

We also measured these branching ratios as a function of temperature over the range 296–475 K, as shown in Figure 3. Unlike our previous study,¹⁷ we find little or no influence of temperature on the branching ratio. We believe that the current study is a more reliable measure of the high-temperature branching ratios because of the better suppression of secondary

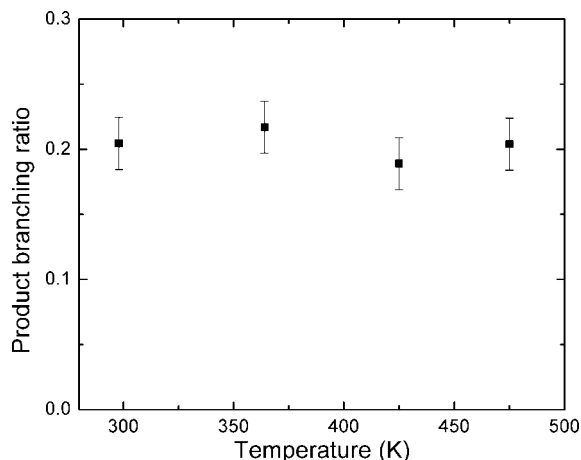
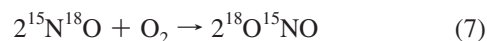


Figure 3. The branching ratio of channel 1b (CO + NO) as a function of temperature.

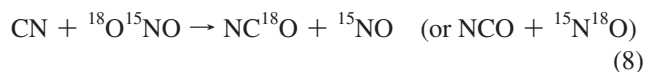
chemistry. In general, branching ratios rarely show a large variation over a small temperature range, such as is available in these experiments. Our measurements are in qualitative agreement with the ab initio calculations of Qu et al.,²² which suggest that the CO + NO channel is accessible via NCO₂ transition states involving a three-member COO ring. Although less favorable than direct dissociation of the bent NCOO complex to form NCO + O, these three-center transition states are still substantially lower in energy than the reactants,²² in contrast to a four-center transition state. Rearrangement to an O–(CON) three-member ring intermediate, which then opens to an O–C–N–O structure, leads to the CO + NO products.

3.2. Secondary Reactions and Kinetics Simulation. Several secondary reactions must be considered. The most important is reaction 2, described above. This reaction represents a potential source of the detected ¹⁴N¹⁶O products. This reaction is expected to be efficiently quenched by small amounts of ¹⁵N¹⁸O reagent; however, at high [¹⁵N¹⁸O], other reactions potentially become important, including the dark reaction between ¹⁵N¹⁸O and O₂:



The rate constant for this reaction (without isotope labeling) is $k_7 = 2.0 \times 10^{-38} \text{ cm}^3 \text{ molec}^{-1} \text{ s}^{-1}$.³⁶ This reaction will proceed very slowly at low ¹⁵N¹⁸O pressures, but at the higher ¹⁵N¹⁸O pressures used, significant amounts of NO₂ (actually ¹⁸O¹⁵N¹⁶O) can be formed over the ~ 7 min time scale for reagent mixing and data collection. Figure 4 shows the calculated concentrations of NO₂ produced in 7 min at different NO pressures. The result shows only 1.5% NO conversion to ¹⁸O¹⁵NO at ¹⁵N¹⁸O = 0.5 Torr, but at ¹⁵N¹⁸O = 4 Torr, the conversion increases to 14%. We have qualitatively observed NO₂ formation under these conditions, as observed by the appearance of a light brown color in the reagent mixture. This indicates that reaction 7 is significant at the higher pressure of ¹⁵N¹⁸O used.

NO₂ formed in reaction 7 can then consume CN radicals:



with a rate constant reported to be $k_8 = 7.8 \times 10^{-11} \text{ cm}^3 \text{ molec}^{-1} \text{ s}^{-1}$.³⁷ Note that although NO is formed in reaction 8, it is not the detected ¹⁴N¹⁶O isotope, and therefore, reactions 7 and 8

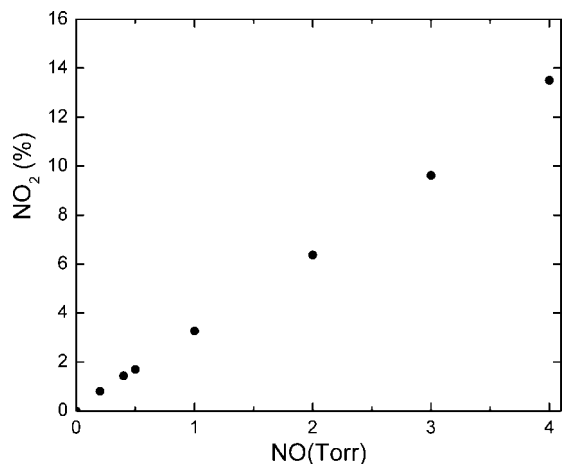


Figure 4. The calculated percent of NO₂ produced from the reaction between O₂ and NO over a 7 min reaction time. $P(\text{O}_2) = 2$ Torr, $P(\text{NO}) = \text{variable}$.

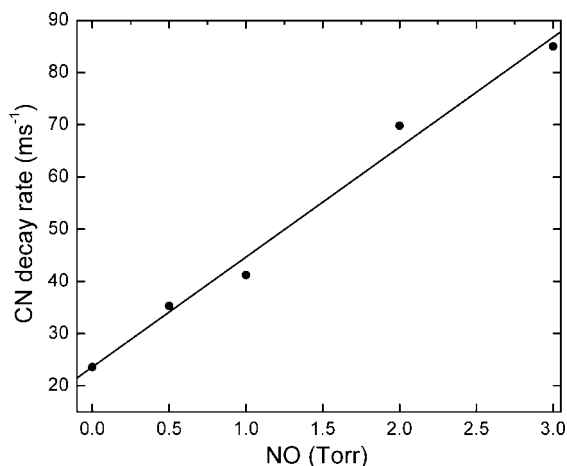


Figure 5. Pseudo-first-order decay rate constant of the CN radical as a function of NO pressure. Reaction conditions: $P(\text{ICN}) = 0.20$ Torr, $P(\text{SF}_6) = 2.0$ Torr, $P(\text{NO}) = \text{variable}$.

represent a mechanism by which the $^{14}\text{N}^{16}\text{O}$ yield would be expected to decrease as the amount of $^{15}\text{N}^{18}\text{O}$ reagent is increased.

A further reaction that needs to be considered is reaction 5. As mentioned above, this is a pressure-dependent reaction, with $k_5 = 1.35 \times 10^{-12} \text{ cm}^3 \text{ molec}^{-1} \text{ s}^{-1}$ at 30 Torr bath gas of Ar and 298 K. At 2 Torr of Ar, k_5 is only $1.25 \times 10^{-13} \text{ cm}^3 \text{ molec}^{-1} \text{ s}^{-1}$.³² We used SF₆ bath gas in our experiment. It is possible that SF₆ is a more efficient stabilizer of vibrationally excited NCNO than N₂. If so, the rate of k_5 in our system may be greater than those in the literature. To examine this possibility, we measured k_5 by CN transient signal detection, and analysis by standard pseudo-first-order kinetics. CN was formed by 266 nm photolysis of ICN and probed using the R(6) line at 2067.91 cm⁻¹. Transient signals were fit to decaying exponentials, and decay rates were plotted as a function of [NO], as shown in Figure 5. The rate constant obtained using 2.0 Torr of SF₆ is $k_5 = (6.23 \pm 1.0) \times 10^{-13} \text{ cm}^3 \text{ molec}^{-1} \text{ s}^{-1}$. This value is substantially greater (about a factor of 4) than that obtained by Wang et al.,³² who used Ar as the bath gas. Although our measurement shows that reaction 5 is, indeed, faster in SF₆ buffer gas, it is still far less competitive for CN radicals than reaction 1a at $P(\text{O}_2) = 2.0$ Torr and $P(^{15}\text{N}^{18}\text{O}) = 0.5$ Torr.

To examine the possible effects of the above secondary chemistry on the experiments, we measured [NO] yields upon

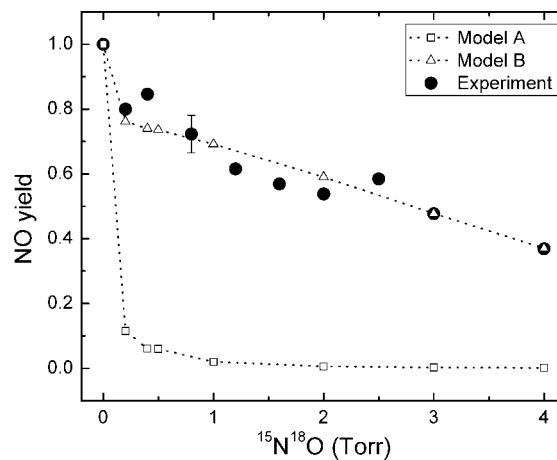


Figure 6. Experimental and simulated dependence of NO yield on added $^{15}\text{N}^{18}\text{O}$ reagent. Experimental results are represented by dots. Model A (squares) assumes that channel 1b is a negligible channel and most of NO originated from secondary chemistry. Model B (triangles) assumes that channel 1b is a significant channel with a branching ratio of 0.20. $P(\text{ICN}) = 0.20$ Torr, $P(\text{O}_2) = 2.0$ Torr, $P(\text{SF}_6) = 2.0$ Torr, $P(^{15}\text{N}^{18}\text{O}) = \text{variable}$. We have assumed that $[\text{CN}]_0 = 3.0 \times 10^{13} \text{ molec cm}^{-3}$ and estimated $[\text{NO}_2]$ from Figure 4.

TABLE 2: Reactions Used in Kinetic Simulation of NO Yield

reaction	k (298 K) $\text{cm}^3 \text{ molec}^{-1} \text{ s}^{-1}$		ref
	model A	model B	
$\text{CN} + \text{O}_2 \rightarrow \text{NCO} + \text{O}$	2.3×10^{-11}	1.84×10^{-11}	this work
$\text{CN} + \text{O}_2 \rightarrow \text{CO} + \text{NO}$	0	0.46×10^{-11}	this work
$\text{NCO} + \text{O} \rightarrow \text{CO} + \text{NO}$	2.1×10^{-10}	2.1×10^{-10}	31
$\text{NCO} + ^{15}\text{N}^{18}\text{O} \rightarrow \text{products}$	3.4×10^{-11}	3.4×10^{-11}	24 ^a
$\text{CN} + ^{15}\text{N}^{18}\text{O} \rightarrow \text{products}$	6.2×10^{-13}	6.2×10^{-13}	this work ^a
$\text{CN} + ^{18}\text{O}^{15}\text{NO} \rightarrow \text{products}$	7.8×10^{-11}	7.8×10^{-11}	37 ^a

^a Rate constants measured using natural isotopic abundance NO and NO₂

photolysis of ICN/O₂/¹⁵N¹⁸O/SF₆ mixtures as a function of ¹⁵N¹⁸O pressure. The data are shown in Figure 6 along with predictions of kinetic modeling simulations, using kinetic data in Table 2. In model simulation A, we assumed that channel 1b is insignificant and that secondary chemistry (primarily reaction 2) is responsible for NO formation. As shown, model A predicts that NO formation is strongly quenched by a small amount of ¹⁵N¹⁸O, primarily by NCO removal (reaction 6a). In model simulation B, however, we assumed that channel 1b has a branching fraction, $\varphi_{1b} = 0.20$, as tentatively determined by assuming that $P(^{15}\text{N}^{18}\text{O}) = 0.5$ Torr is sufficient to suppress reaction 2 but insufficient to significantly compete for CN radicals (reaction 5 and 8). As shown, model B predicts only a small drop in NO yield at 0.5 Torr ¹⁵N¹⁸O, but a gradual decrease in [NO] as ¹⁵N¹⁸O pressure is increased to several Torr. We attribute the slow decay primarily to reaction 8, reaction of CN with NO₂ produced by the dark reaction of O₂ and ¹⁵N¹⁸O. We note that removal of reaction 5 from model B resulted in virtually no change in the results. Most importantly, the experimental data are in excellent agreement with model B, and are clearly not consistent with model A. Furthermore, we note that at $P(^{15}\text{N}^{18}\text{O}) = 0.5$ Torr, the pressure used in Figure 2, reaction 2 is, indeed, almost completely suppressed, as expected. On this basis, we can conclude with a high degree of confidence that channel 1b is in fact a significant (albeit not dominant) channel of the CN + O₂ reaction.

4. Conclusion

Infrared absorption spectroscopy was used to investigate the product channel of CN + O₂ reaction. Detection and quantification of NO products along with kinetic modeling simulations show that the CO + NO is a significant channel with a branching ratio of 0.20 ± 0.02 . The branching ratio was found to be independent of temperature over the range $T = 296\text{--}475$ K.

Acknowledgment. This work was supported by the Division of Chemical Sciences, Office of Basic Energy Sciences of the Department of Energy, Grant DE-FG03-96ER14645.

References and Notes

- (1) Phillips, L. F.; Smith, I. W. M.; Tuckett, R. P.; Whitham, C. J. *Chem. Phys. Lett.* **1991**, *183*, 254.
- (2) Schmatjko, K. J.; Wolfrum, J. *Ber. Bunsen-Ges. Phys. Chem.* **1978**, *82*, 419.
- (3) Wright, S. A.; Dagdigian, P. J. *J. Chem. Phys.* **1995**, *100*, 6479.
- (4) Reisler, H.; Mangir, M.; Wittig, C. *Chem. Phys.* **1980**, *47*, 49.
- (5) Jensen, R. C.; Walton, D. B.; Coombe, R. D. *Ber. Bunsen-Ges. Phys. Chem.* **1990**, *169*, 441.
- (6) Anastasi, C.; Hancock, D. U. *J. Chem. Soc., Faraday Trans. 2* **1988**, *84*, 9.
- (7) Lichtin, D. A.; Lin, M. C. *Chem. Phys.* **1985**, *96*, 473.
- (8) Louge, M. Y.; Hanson, R. K. *Int. J. Chem. Kinet.* **1984**, *16*, 231.
- (9) You, Y. Y.; Wang, N. S. *J. Chin. Chem. Soc. (Taipei)* **1993**, *40*, 337.
- (10) Durant, J. L., Jr.; Tully, F. P. *Chem. Phys. Lett.* **1989**, *154*, 568.
- (11) Balla, R. J.; Castleton, K. H. *J. Phys. Chem.* **1991**, *95*, 2344.
- (12) Baulch, D. L.; Cobos, C. J.; Cos, R. A.; Frank, P.; Hayman, G.; Just, Th.; Kerr, J. A.; Murrells, T.; Pilling, M. J.; Troe, J.; Walker, R. W.; Warnatz, J. *J. Phys. Chem. Ref. Data* **1994**, *23* (Suppl. 1), 847.
- (13) Sims, I. R.; Queffelec, J.-L.; Defrance, A.; Rebrion-Rowe, C.; Travers, D.; Bocherel, P.; Rowe, B. R.; Smith, I. W. M. *J. Chem. Phys.* **1994**, *100*, 4229.
- (14) Atakan, B.; Jacobs, A.; Wahl, M.; Weller, R.; Wolfrum, J. *Chem. Phys. Lett.* **1989**, *154*, 449.
- (15) Burmeister, M.; Gulati, S. K.; Natarajan, K.; Thielen, K.; Mozzhukin, E.; Roth, P. *Symp. (Int.) Combust. (Proc.)* **1989**, *22*, 1083.
- (16) Smith, I. W. M. In *Chemical Dynamics and Kinetics of Small Radicals*; Liu, K., Wagner, A. Eds.; World Scientific: Singapore, 1995; Part I, p 214.
- (17) Rim, K. T.; Hershberger, J. F. *J. Phys. Chem. A* **1999**, *103*, 3721.
- (18) Witinski, M. F.; Ortiz-Suárez, M.; Davis, H. F. *J. Chem. Phys.* **2006**, *124*, 94307.
- (19) Vallance, C.; Maclagan, R. G. A. R.; Phillips, L. F. *Chem. Phys. Lett.* **1996**, *250*, 59.
- (20) Klippenstein, S. J.; Kim, T.-W. *J. Chem. Phys.* **1993**, *99*, 5790.
- (21) Phillips, L. F. *J. Phys. Chem. A* **1998**, *102*, 31.
- (22) Qu, Z.; Zhu, H.; Li, Z.; Zhang, X.; Zhang, Q. *Chem. Phys. Lett.* **2002**, *353*, 304.
- (23) Smith, I. W. M. *Int. J. Mass Spectrom. Ion Processes* **1995**, *149*, 231.
- (24) Cooper, W. F.; Park, J.; Hershberger, J. F. *J. Phys. Chem.* **1993**, *97*, 3283.
- (25) Mohammad, F.; Morris, V. R.; Fink, W. H.; Jackson, W. M. *J. Phys. Chem.* **1993**, *97*, 11590.
- (26) Chambreau, S. D.; Townsend, D.; Lahankar, S. A.; Lee, S. K.; Suits, A. G. *Phys. Scr.* **2006**, *73*, C89.
- (27) Chambreau, S. D.; Lahankar, S. A.; Suits, A. G. *J. Chem. Phys.* **2006**, *125*, 044303.
- (28) Lahankar, S. A.; Chambreau, S. D.; Suits, F.; Farnum, J.; Zhang, X.; Bowman, J. M.; Suits, A. G. *J. Chem. Phys.* **2006**, *125*, 044302.
- (29) Lahankar, S. A.; Chambreau, S. D.; Zhang, X.; Bowman, J. M.; Suits, A. G. *J. Chem. Phys.* **2007**, *126*, 044314.
- (30) Suits, A. G.; Chambreau, S. D.; Lahankar, S. A. *Int. Rev. Phys. Chem.* **2007**, *26*, 585.
- (31) Gao, Y.; Macdonald, R. G. *J. Phys. Chem. A* **2003**, *107*, 4625.
- (32) Wang, N. S.; Yang, D. L.; Lin, M. C. *Chem. Phys. Lett.* **1989**, *163*, 480.
- (33) Cooper, W. F.; Hershberger, J. F. *J. Phys. Chem.* **1992**, *96*, 771.
- (34) Cooper, W. F.; Hershberger, J. F. *J. Phys. Chem.* **1992**, *96*, 5405.
- (35) Rothman, L. S.; et al. *J. Quant. Spectrosc. Radiat. Transfer* **1992**, *4*, 8–469.
- (36) Wooldridge, S. T.; Mertens, J. D.; Hanson, R. K.; Bowman, C. T. *Symp. Int. Combust. Processes* **1994**, *25*, 983.
- (37) Atkinson, R.; Baulch, D. L.; Cox, R. A.; Crowley, J. N.; Hampson, R. F.; Hynes, R. G.; Jenkin, M. E.; Rossi, M. J.; Troe, J. *Atmos. Chem. Phys.* **2004**, *4*, 1461.

JP811364K